Available online at www.sciencedirect.com

jmr&t Journal of Materials Research and Technology

journal homepage: www.elsevier.com/locate/jmrt

Original Article

A novel method for the spring-back analysis of a hot stamping steel

Melwin Sajan[*], *M. Amirthalingam*, *Uday Chakkingal*

Department of Metallurgical and Materials Engineering, Indian Institute of Technology Madras, Chennai, 600 036, India

ARTICLE INFO

Article history:
Received 5 December 2020
Accepted 5 January 2021
Available online 13 January 2021

Keywords:
Hot stamping
Advanced high strength steels
Cooling rate
V-bending
Spring-back
Phase transformation

ABSTRACT

Spring-back of sheet metal affects the dimensional accuracy of the components after stamping and has to be eliminated or corrected. Advanced high strength steels (AHSS) are prone to spring-back while forming at ambient temperatures. Hot stamping process is an effective technique to reduce the spring-back upon forming. The forming temperatures and the phase transformations associated with quenching are known to influence the spring-back. However, the detailed experimental analysis on spring-back behaviour is limited due to the difficulty in physically simulating the thermal-mechanical conditions prevailing in a typical hot forming process. In the present work, a novel V-bending technique is presented for effectively measuring the spring-back using a thermal-mechanical simulator, Gleeble™. V-bending is carried out by applying a compressive force along the longitudinal plane of AHSS steel strips at forming temperatures. Upon V-bending, samples were cooled at different cooling rates while maintaining the forming loads to simulate die quenching. Results indicate that the spring-back decreases and becomes close to zero (at a cooling rate of 20 K s^{-1}) with an increase in cooling rate for a hot stamping steel. Further, an increase in cooling rate results in spring-forward owing to the formation of an increased volume fraction of martensite.

1. Introduction

The automotive industry demands processing techniques to produce high strength sheet metal components with good dimensional accuracy [1–3]. It is known that an increase in the yield strength of the material increases the elastic recovery (spring-back) after forming which in turn affects the dimensional accuracy of the component [4–7]. Spring-back is proportional to the ratio of yield stress to Young's modulus of the material [7]. Hot stamping is seen as an attractive process to reduce the spring-back and forming load during the forming of advanced high strength steels (AHSS) [8–12]. In a hot stamping process, steel with boron addition is formed in the austenitic region and subsequently quenched in the die to produce high strength martensitic microstructures [9,13–16]. A reduction of 5°–6° in the spring-back angle can be achieved by using the hot stamping process instead of stamping at ambient temperatures [17]. It is reported that the interplay

* Corresponding author.
E-mail address: melwinms@gmail.com (M. Sajan).
https://doi.org/10.1016/j.jmrt.2021.01.017

between forming temperatures and solid-state phase transformations leads to a reduction in spring-back [4,5,18,19]. However, the exact mechanism by which these parameters influence the spring back is not yet clearly understood. Therefore, it is desirable to be able to physically simulate the thermal-mechanical conditions in a hot forming process under different forming conditions and study the resultant spring-back.

Forming temperature is one of the reasons for the reduction in spring-back in a hot stamping process [4,5]. The influence of forming temperature on spring-back in steel (DP 600 and mild steel) was studied in a hot compression testing machine by Yanagimoto et al. [4]. V-bending was carried out at various temperatures in a die with the aid of an induction heater and PID controller. It was reported that as the forming temperature increased from 298 K to 873 K, the spring-back decreased. It was stated that the considerable reduction in spring back above 750 K was due to the recrystallisation of ferrite grains [4]. Yanagimoto and Oyamada [5] conducted experiments by tensile loading and unloading to clarify the mechanism of the reduction in spring-back while forming at a temperature above 750 K and speculated that creep strain at high temperature is a secondary reason for the reduction in spring-back. However, the exact mechanism by which creep strain contributes to the spring-back is not fully understood. Even though the strain state in the hot stamping process can be complex, all fundamental studies on the evaluation of spring-back use V-shaped or U-shaped dies for spring-back measurements [4,5,19,20]. The conventional punch-die techniques enable investigation of different forming temperatures on the spring-back; however, the effect of different cooling rates on the resultant spring back cannot be easily replicated.

It is well known that the cooling rate in a hot stamping process dictates the phase transformations and resultant microstructure of the stamped component [21–25]. Lee et al. [18] investigated the role of transformation plasticity on spring-back by incorporating transformation kinetics and transformation plastic theory in a three-point bending model using finite element analysis. In their simulations, the bend samples were cooled to room temperature at a cooling rate of 5 K s^{-1} and 50 K s^{-1} to form bainitic and martensitic microstructure respectively. It was reported that the spring-back was reduced from 11.5% to 4.5% on increasing the cooling rate from 5 K s^{-1} to 50 K s^{-1}. This indicated that the transformation plasticity along with the forming temperature has a significant role in reducing the spring-back in a hot stamping process. However, the quantitative and experimental analysis of the spring-back with varying cooling rates and resultant phase transformations is limited owing to the absence of a temperature and cooling rate controlled spring-back analysis system. Nakagawa et al. [19] studied the influence of phase transformations on the spring-back behaviour by varying the die quenching time (0, 3 and 10 s) after forming in a 22MnB5 steel. The sample was austenitised in a furnace and transferred manually to a hat-shaped bending die to form and quench. It was observed that the spring-back was 3° more for samples without die quenching than the samples with a die quenching time of 10 s indicating a reduction in the spring-back with martensitic transformation. However, the experimental setup failed to account for the effect of temperature drop in the material during the manual transfer from the furnace to die and drop of flange temperature during forming. Moreover, the lack of a proper feedback system to control the cooling rate resulted in ambiguity in interpretation. Therefore, it is desirable to develop a new method of V-bending with excellent temperature and cooling rate control to address the influence of the cooling rate and resultant phase transformation on spring-back in a hot stamping process. The present work introduces a novel V-bending technique for analysing the mechanism of reduction in the spring-back and material behaviour during hot stamping by physically simulating the thermal-mechanical conditions on a laboratory scale. While this does not directly simulate the industrial hot stamping process, simple experimental determination of spring-back can help in identifying potential problems during industrial hot stamping under varying hot stamping temperatures, and cooling rates imposed during die quenching.

2. Materials and methods

The chemical composition of the hot stamping steel used for the study is given in Table 1. In this work, a novel method has been used to simulate the isothermal hot stamping process using V-bending experiments in a Gleeble™ at austenitising temperatures. The schematic diagram of the novel V-bending experimental method is shown in Fig. 1 and the experimental setup for the V-bending study is shown in Fig. 2. For the V-bending tests, steel strips of dimension 120 × 25.4 × 2 mm^3 were clamped between the jaws of Gleeble™. The length of gripping region was 30 mm on both ends and the gripping force was maintained constant throughout the experiment. Three thermocouples were attached to the samples at points A (center), B (7 mm from center) and C (14 mm from center) as in Fig. 1 for recording the temperature. The temperature of the specimen is controlled by the thermocouple at the center (A) and a temperature feedback system in Gleeble™. Specimens were heated to a temperature in the austenite region (1173 K) at a heating rate of 10 K s^{-1} by Joule heating and soaked for 300 s to ensure complete austenitisation. V-bending was carried out at this temperature by moving one jaw towards the other jaw which was fixed. The axial compressive force causes the specimens to buckle and form a V-bend. The samples were deformed by a compressive stroke of 80 mm with a stroke rate of 0.5 mm s^{-1} to produce a V-bend. The use of a die-punch assembly which will limit the range of cooling rates that can be investigated is therefore eliminated. After this V bending, the specimen was subsequently cooled to room temperature under axial compressive load with various cooling rates (10, 15, 20, 25, 30, 50 and 70 K s^{-1}), by compressed air quenching. The cooling rate was controlled by the combined action of Joule heating, temperature feedback system and compressed air quenching system of the Gleeble™. After cooling to room

Table 1 – Chemical composition (weight percentage) of hot stamping steel, as-received.

% C	% Mn	% Si	% Ti	% Al	% B	% Cr	% P
0.23	1.17	0.26	0.04	0.04	0.0029	0.17	0.01

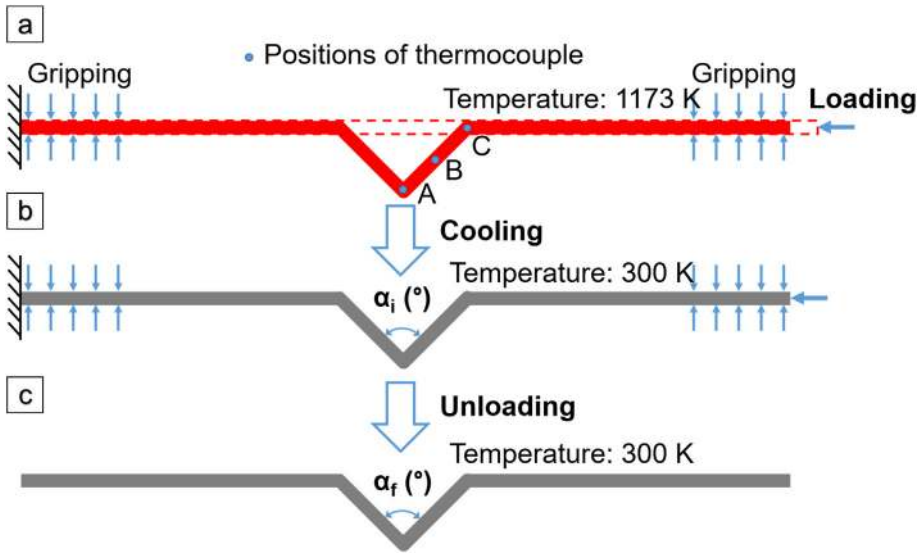

Fig. 1 – Schematic diagram of the V-bending test in Gleeble™; (a) V-bending at 1173 K by applying compressive force, (b) Cooling under compressive force to room temperature at various cooling rates and V-bend angle is measured at 300 K and (c) Load is removed to measure final V-bend angle.

temperature, images of the quenched V-bending specimen with load and after unloading were captured to measure the spring-back angle. In an actual hot stamping process, cooling rates generally vary along the whole section of the component due to the complex shapes of a die. Therefore, the experimental methodology used here presents a physical correlation between the novel V-bending test and the hot stamping process. The microstructure at the bend region (cross-section) of the V-bend samples was obtained by using an optical microscope after etching with 2% Nital.

To determine the volume fraction of phases formed with the selected cooling rates (10, 15, 20, 25, 30, 50 and 70 K s^{-1}), dilatation measurements were carried out in Gleeble™ on steel strips of 180 × 48 × 2 mm^3 (Gleeble™ standard). The strips were heated to 1173 K with the same heating and soaking conditions that were used for V-bending in Gleeble™ with a dilatometer attached at the center in the transverse direction. The strips were then cooled from 1173 K with various cooling rates and the dilatation was recorded.

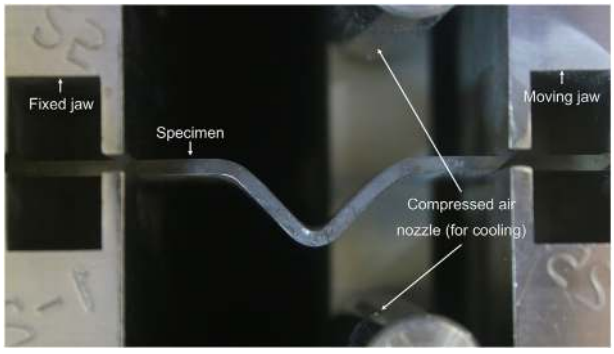

Fig. 2 – Image of the experimental setup for V-bending under various cooling rates.

3. Results and discussion

The temperature–time history (at the center of the strip, A) of the V-bending experiments is shown in Fig. 3. The temperature history of the specimen is maintained identical throughout the experiments up to the end of the V-bending by using a temperature feedback system in Gleeble™. The cooling rate of the process is accurately controlled with a maximum deviation of 1 K s^{-1} from the target cooling rate. However, a temperature gradient is observed along the length of the V-bending specimen during austenitisation which is shown in Fig. 4 (image of a V-bending sample with load and after unloading). A difference in temperature of 5 K is observed between points A and B which are 7 mm apart. The points D and B in Fig. 4 are assumed to be at the same temperature since they are equidistant from the center point A

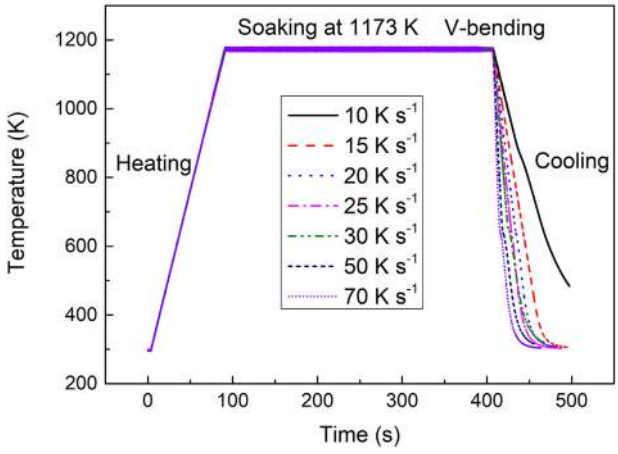

Fig. 3 – Temperature - time history (at the center of the strip, A) of the V-bending experiments.

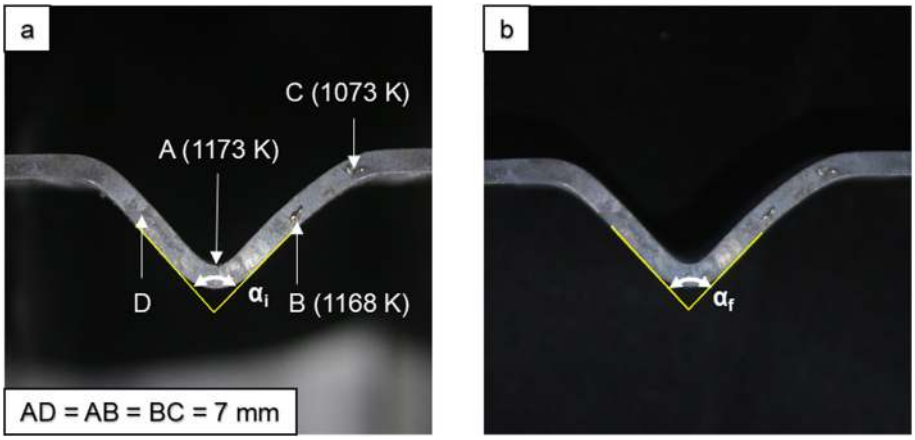

Fig. 4 – Images of V-bend samples for the cooling rate of 10 K s^{-1} (a) with load and (b) after unloading.

and the grips. Therefore, the region where the bend angle is measured (D to B in Fig. 4) can be assumed to be within acceptable temperature difference (5 K). Since the bending is carried out at the same austenitisation temperature (1173 K at A) in all experiments, the influence of this temperature gradient on the study of the effect of cooling rate on spring-back can be neglected. The deformation on the left and right side arms of the V-bend is found to be symmetric along the vertical axis through A in the region where the bend angle is measured (D to B in Fig. 4) due to homogeneous temperature distribution. However, there is a negligible asymmetry in deformation is found along the vertical axis through A beyond points D and B, due to possible prevailing temperature gradient. As this asymmetry is away from the region where the V-bend angle is measured (between D to B), the accuracy of measured spring-back is unaffected.

The V-bend angles before and after unloading are measured using an image analysis software, ImageJ, to quantify the spring-back behaviour. The spring-back angle, as well as spring-back ratio, is calculated from the images of the sample with load (measured angle is α_i, Fig. 4a) and after unloading (measured angle is α_f, Fig. 4b) and presented in Table 2. The amount of Spring-back angle is the difference between the bend angles before and after unloading [4,7].

$$\text{Spring} - \text{back angle}, \alpha = \alpha_f - \alpha_i \quad (1)$$

$$\text{Spring} - \text{back ratio}, K = \frac{\alpha_f}{\alpha_i} \quad (2)$$

The spring-back angle is found to be decreasing with increasing cooling rate. The spring-back angle which is 1.15° at a cooling rate of 10 K s^{-1}, decreases to 0.21° at a cooling rate of 20 K s^{-1}. Moreover, the spring-back changes its direction from positive spring-back (outward opening up of the V bend angle) to negative spring-back or spring-forward (inward closing up of the V bend angle) at cooling rated 25 K s^{-1} and higher. At these cooling rates, it is observed that the spring-back has remained unchanged with a value of about −0.6°. The phenomenon causing this variation in the spring-back angle is further investigated using microstructural analysis and dilatometry study.

The microstructure at the bend region (cross-section) of the V-bend samples is shown in Fig. 5. From the microstructure, it can be confirmed that the transformation product at a cooling rate of 10 K s^{-1} is ferrite/pearlite and a cooling rate of 25 K s^{-1} give a fully martensitic microstructure. Therefore, it can be concluded that the critical cooling rate which is required for the complete martensite transformation of the steel in the present study is 25 K s^{-1}. Laths of martensite are found on the samples cooled at a rate of 15 K s^{-1} and above. For a cooling rate of 15 K s^{-1} and 20 K s^{-1}, a mixed microstructure with pearlite, bainite and martensite is observed.

Dilatometry study is carried out in Gleeble™ to measure the volume fraction of phase formed with the selected cooling rates (10, 15, 20, 25, 30, 50 and 70 K s^{-1}). Phase transformations are associated with a change in volume which is observed as a function of temperature in the dilatometry study [26].

Table 2 – Spring-back angle for various cooling rates.

Cooling rate (K s^{-1})	Martensite volume fraction (%)	Loaded v-bend angle,α_i (°)	Unloaded v-bend angle, α_f (°)	Spring-back angle, α (°)	Spring-back ratio, K
10	0	86.93	88.08	1.15	1.01
15	35 ± 9	86.01	86.64	0.63	1.01
20	74 ± 5	85.31	85.52	0.21	1.00
25	100	87.04	86.48	−0.56	0.99
30	100	85.99	85.44	−0.55	0.99
50	100	84.39	83.75	−0.64	0.99
70	100	86.99	86.38	−0.61	0.99

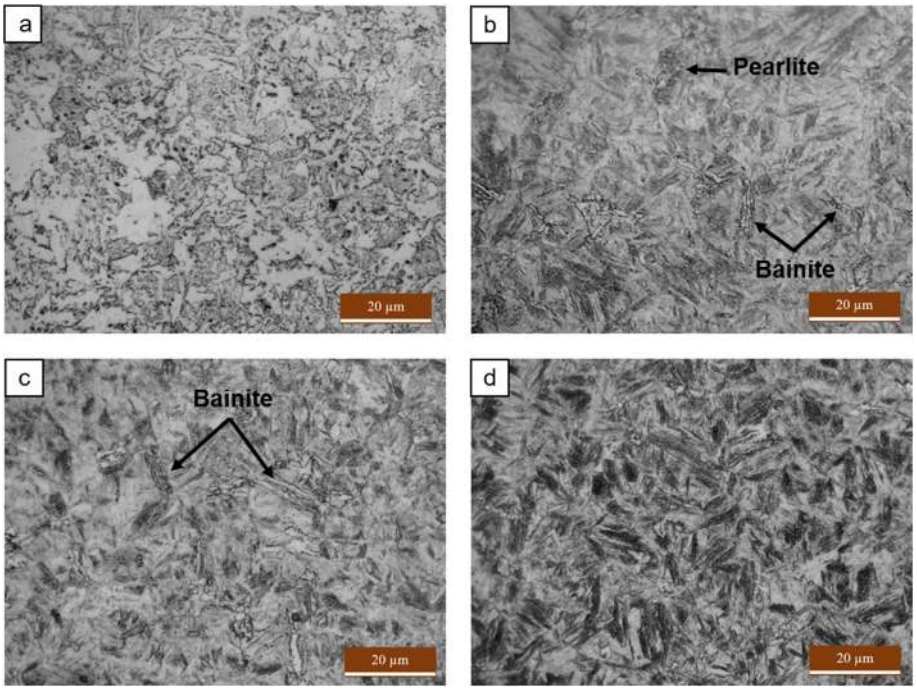

Fig. 5 – Microstructure of the V-bend samples after quenching with various cooling rates; (a) 10 K s^{-1} (b) 15 K s^{-1} (c) 20 K s^{-1} and (d) 25 K s^{-1}.

Dilatation curves obtained for the above-mentioned cooling rates are shown in Fig. 6. Though the austentisation temperature is 1173 K, the dilatation cooling curves are plotted from 1120 K to eliminate initial disturbance and serrations in the dilatation during the onset of cooling cycles (due to blowing of compressed air). It is assumed that the dilatation behaviour is linear above 1120 K due to the absence of any phase transformations. Dilatation curves are evaluated by the method described by Motycka et al. [27]. Austenite transformation temperatures (1% of austenite and 99% of austenite) were measured from the change in the slope of dilatation and are shown in Table 3. The phase transformation products are identified by comparing the transformation temperatures and nature of dilatation curves with existing studies in the hot stamping steels [1,21,28,29]. Dilatation curves with single and multiple phase transformations are observed for various cooling rates. At a cooling rate of 10 K s^{-1}, single-phase transformation is observed, where austenite decomposition starts at a temperature 893 K and ends at a temperature above 700 K, which indicates the formation of high-temperature transformation products such as ferrite and pearlite. As the cooling rate increases (15 and 20 K s^{-1}) multiple transformations are observed and the austenite decomposition is completed at about 500 K which shows the formation of pearlite/bainite as well as martensite. At higher cooling rates (25, 30, 50 and 70 K s^{-1}), again single-phase transformation is seen, confirming only martensite formation from austenite. Moreover, austenite decomposition start temperature is reduced as the cooling rate increases and it becomes constant from 25 K s^{-1} onwards, which substantiates complete martensitic transformation at that cooling rate (Table 3).

Table 3 – Austenite decomposition temperatures for different cooling rates.

Cooling rate (K s^{-1})	Austenite decomposition start temperature (K)	Austenite decomposition end temperature (K)
10	893 ± 2	708 ± 10
15	855 ± 10	555 ± 10
20	854 ± 9	531 ± 3
25	646 ± 19	515 ± 2
30	656 ± 19	518 ± 6
50	642 ± 15	517 ± 3
70	659 ± 6	512 ± 6

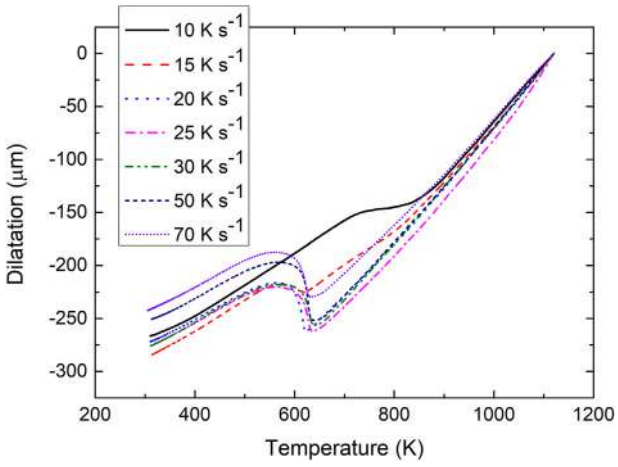

Fig. 6 – Dilatation curves for the cooling rates 10, 15, 20, 25, 30, 50 and 70 K s^{-1}.

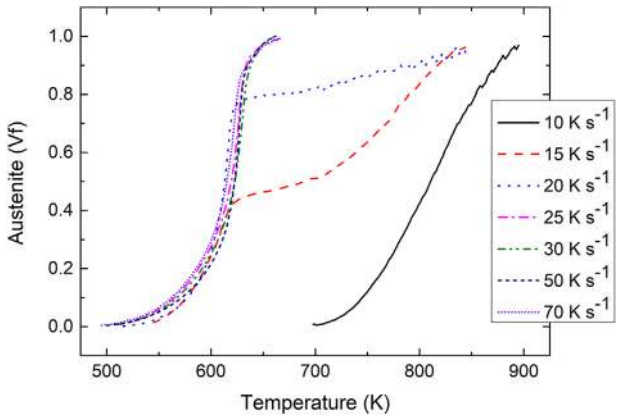

Fig. 7 – Austenite volume fraction as a function of temperature under various cooling rates.

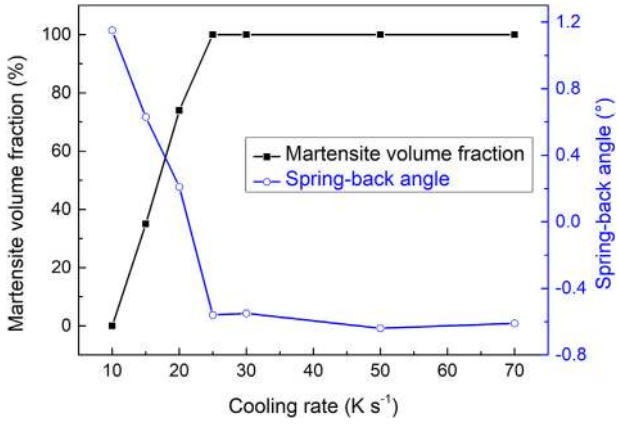

Fig. 8 – Martensite volume fraction and spring-back angle for various cooling rates.

Therefore, it can be confirmed that the critical cooling rate of the steel in the present study is 25 K s^{-1}.

Austenite volume fraction has been calculated as a function of cooling rates by using lever rule as described by Mohanty et al. [26] and Motycka et al. [27]. Fig. 7 shows the volume fraction of austenite as a function of temperature for various cooling rates. The volume fraction of martensite (low-temperature transformation product) for each cooling rate was identified from the austenite volume fraction curve and tabulated (Table 2). As the cooling rate increases, the volume fraction of martensite is found to be increased, until the critical cooling rate where the microstructure is completely martensite.

The reduction in the spring-back angle with an increase in the cooling rate can be correlated with the volume fraction of martensite after quenching (Fig. 8). The spring-back reduces with an increase in the volume fraction of martensite. For a cooling rate of 10 K s^{-1}, there is no formation of martensite and has the highest spring-back angle (1.15°) among the selected cooling rates. The spring-back angle reaches the least positive value (0.21°) when the volume fraction of martensite becomes 74% at a cooling rate of 20 K s^{-1}. The spring-back ratio is almost 1 at this cooling rate, indicates that there is no elastic recovery after unloading and suitable condition for spring-back free bending. At the critical cooling rate of the material (25 K s^{-1}), the phenomenon of spring-forward or negative spring-back is observed and above the critical cooling rate, the spring-back angle does not change since the microstructure is completely martensite. It also confirms that the reduction in the spring-back with an increase in the cooling rate solely depends on the volume fraction of martensite formed. It is well known that volume expansion occurs during martensitic transformation [19]. It can therefore be concluded that the volume expansion and associated transformation strain developed with the austenite to martensite transformation is the reason for the reduction in the spring-back. It is reported that the stress induced by hot stamping is released during martensite transformation resulting in the lowering of spring-back [18]. The transformation strain counters the elastic recovery of the material and thus spring-back is reduced. However, the phenomenon of spring-forward at a cooling rate of 25 K s^{-1} and above, due to the formation of 100% of martensite is undesirable.

4. Conclusion

A novel V bending technique to simulate the thermal-mechanical conditions prevailing in a hot stamping process has been developed using the Gleeble™, thermal-mechanical simulator. Using this technique, the influence of cooling rates and phase transformations on spring-back is understood for a hot stamping steel. From this work, the following conclusions are drawn:

- The cooling rate has a significant role in determining the spring-back in a hot stamping process for a given austenitisation temperature. Spring-back can be reduced to zero by controlling the cooling rate of the process by altering the microstructural constituents favourably.
- For an AHSS under investigation (0.23C-1.17Mn-0.26Si-0.0029 B, wt. %), spring back reduces to a value close to zero (0.21°) from 1.15° by an increase in the cooling rate from 10 K s^{-1} to 20 K s^{-1}. A further increase in the cooling rate results in a spring-forward phenomenon and reaches a value of −0.6°.
- Above a critical cooling rate (25 K s^{-1}), cooling rate does not affect the spring-back behaviour, for the material under investigation, due to complete martensite formation.
- The increase in the volume fraction of martensite with an increase in the cooling rate is the primary reason for the reduction in the spring-back, owing to the transformation plasticity associated with the martensite transformation.
- The novel V-bending technique by compressive load in Gleeble™ is established as an easy and reliable

methodology for analysing the spring-back behaviour while applying thermal-mechanical cycles of a hot stamping process.

Funding

This study was funded by the Department of Science and Technology, Government of India, under Extra Mural Research grant (EMR/2016/001791).

Data availability

The raw/processed data required to reproduce these findings cannot be shared at this time as the data also forms part of an ongoing study.

Declaration of Competing Interest

The authors declare that they have no known competing financial interests or personal relationships that could have appeared to influence the work reported in this paper.

Acknowledgement

We thank ArcelorMittal for providing hot stamping steels for the study. The authors also acknowledge the financial support of the Department of Science and Technology, Government of India through FIST program (Grant no: SR/FST/ETII-049) for establishing a Gleeble™ thermo-mechanical simulation facility at IIT Madras.

REFERENCES

[1] Åkerström P, Wikman B, Oldenburg M. Material parameter estimation for boron steel from simultaneous cooling and compression experiments. Model Simulat Mater Sci Eng 2005;13:1291–308. https://doi.org/10.1088/0965-0393/13/8/007.

[2] Matlock DK, Speer JG. Processing opportunities for new advanced high-strength sheet steels. Mater Manuf Process 2010;25:7–13. https://doi.org/10.1080/10426910903158272.

[3] Gracia-Escosa E, García I, Damborenea JJD, Conde A. Friction and wear behaviour of tool steels sliding against 22MnB5 steel. J Mater Res Technol 2017;6:241–50. https://doi.org/10.1016/j.jmrt.2017.04.002.

[4] Yanagimoto J, Oyamada K, Nakagawa T. Springback of high-strength steel after hot and warm sheet formings. CIRP Ann 2005;54:213–6. https://doi.org/10.1016/S0007-8506(07)60086-9.

[5] Yanagimoto J, Oyamada K. Mechanism of springback-free bending of high-strength steel sheets under warm forming conditions. CIRP Ann 2007;56:265–8. https://doi.org/10.1016/j.cirp.2007.05.099.

[6] Ozturk F, Ece RE, Polat N, Koksal A. Effect of warm temperature on springback compensation of titanium sheet. Mater Manuf Process 2010;25:1021–4. https://doi.org/10.1080/10426914.2010.492056.

[7] Mori K, Akita K, Abe Y. Springback behaviour in bending of ultra-high-strength steel sheets using CNC servo press. Int J Mach Tool Manufact 2007;47:321–5. https://doi.org/10.1016/j.ijmachtools.2006.03.013.

[8] Neugebauer R, Altan T, Geiger M, Kleiner M, Sterzing A. Sheet metal forming at elevated temperatures. CIRP Ann 2006;55:793–816. https://doi.org/10.1016/j.cirp.2006.10.008.

[9] Merklein M, Lechler J. Investigation of the thermo-mechanical properties of hot stamping steels. J Mater Process Technol 2006;177:452–5. https://doi.org/10.1016/j.jmatprotec.2006.03.233.

[10] Naderi M, Saeed-Akbari A, Bleck W. The effects of non-isothermal deformation on martensitic transformation in 22MnB5 steel. Mater Sci Eng, A 2008;487:445–55.

[11] Karaağaç İ, Önel T, Uluer O. The effects of local heating on springback behaviour in v bending of galvanized DP600 sheet. Ironmak Steelmak 2019;47:807–13. https://doi.org/10.1080/03019233.2019.1615308.

[12] Lu L, Liang Z, Yang J, Sun Q, Zhu T, Wang X. Investigation on laser welding of a novel hot-stamped steel with 2000 MPa. Journal of Materials Research and Technology 2020;9:13147–52. https://doi.org/10.1016/j.jmrt.2020.09.044.

[13] Vaissiere L, Laurent JP, Reinhardt A. Development of pre-coated boron steel for applications on PSA peugeot citroën and RENAULT bodies in white. SAE Technical Papers 2002;111:909–17. https://doi.org/10.4271/2002-01-2048.

[14] Karbasian H, Tekkaya AE. A review on hot stamping. J Mater Process Technol 2010;210:2103–18.

[15] Hung TH, Wang SW, ChiuHuang CK, Chen FK. Performance of die cooling system design in hot stamping process. J Chinese Ins Eng, Transac Chinese Ins Eng,Series A 2019;42:479–87. https://doi.org/10.1080/02533839.2019.1611477.

[16] Bao L, Liu WJ, Wang B, Li H, You X, Zhou Q, et al. Experimental investigation on partition controllable induction heating-hot stamping process of high-strength boron alloyed steel plates with designable temperature patterns. J Mater Res Technol 2020;9:13963–76. https://doi.org/10.1016/j.jmrt.2020.09.134.

[17] Ikeuchi K, Yanagimoto J. Valuation method for effects of hot stamping process parameters on product properties using hot forming simulator. J Mater Process Technol 2011;211:1441–7.

[18] Lee MG, Kim SJ, Han HN. Finite element investigations for the role of transformation plasticity on springback in hot press forming process. Comput Mater Sci 2009;47:556–67. https://doi.org/10.1016/j.commatsci.2009.09.024.

[19] Nakagawa Y, Mori K, Maeno T. Springback-free mechanism in hot stamping of ultra-high-strength steel parts and deformation behaviour and quenchability for thin sheet. Int J Adv Manuf Technol 2018;95:459–67. https://doi.org/10.1007/s00170-017-1203-3.

[20] Umur Y, Aydin H, Yigit K, Bayram A. Springback/springforward behaviour of DP steels used in the automotive industry. Teh Vjesn 2020;27:243–50. https://doi.org/10.17559/TV-20181004144024.

[21] Bardelcik A, Salisbury CP, Winkler S, Wells MA, Worswick MJ. Effect of cooling rate on the high strain rate properties of boron steel. Int J Impact Eng 2010;37:694–702.

[22] Nishibata T, Kojima N. Effect of quenching rate on hardness and microstructure of hot-stamped steel. J Alloys Compd 2013;577:S549–54.

[23] Cavusoglu O, Cavusoglu O, Yilmazoglu AG, Uzel U, Aydin H, Güral A. Microstructural features and mechanical properties of 22MnB5 hot stamping steel in different heat treatment

conditions. J Mater Res Technol 2020;9:10901–8. https://doi.org/10.1016/j.jmrt.2020.07.043.

[24] Liu S, Long M, Zhang S, Zhao Y, Zhao J, Feng Y, et al. Study on the prediction of tensile strength and phase transition for ultra-high strength hot stamping steel. J Mater Res Technol 2020;9:14244–53. https://doi.org/10.1016/j.jmrt.2020.10.043.

[25] Da Costa Ximenes DA, Moreira LP, De Carvalho JER, Leite DNF, Toledo RG, Da Silva Dias FM. Phase transformation temperatures and Fe enrichment of a 22MnB5 Zn-Fe coated steel under hot stamping conditions. J Mater Res Technol 2020;9:629–35. https://doi.org/10.1016/j.jmrt.2019.11.003.

[26] Mohanty RR, Girina OA, Fonstein NM. Effect of heating rate on the austenite formation in low-carbon high-strength steels annealed in the intercritical region. Metall Mater Trans 2011;42:3680–90. https://doi.org/10.1007/s11661-011-0753-5.

[27] Motyčka P, Kövér M. Evaluation methods of dilatometer curves of phase transformations. In: 2nd Int. Conf. Recent Trends Struct. Mater. Park. Plzen, Czech Repub. COMAT 2012; 2012. p. 2–8.

[28] Naderi M, Durrenberger L, Molinari A, Bleck W. Constitutive relationships for 22MnB5 boron steel deformed isothermally at high temperatures. Mater Sci Eng, A 2008;478:130–9. https://doi.org/10.1016/j.msea.2007.05.094.

[29] Mun DJ, Shin EJ, Choi YW, Lee JS, Koo YM. Effects of cooling rate, austenitizing temperature and austenite deformation on the transformation behavior of high-strength boron steel. Mater Sci Eng, A 2012;545:214–24. https://doi.org/10.1016/j.msea.2012.03.047.